Compact fiber laser for 589 nm laser guide star generation

D. M. Pennington, J. W. Dawson, R.J. Beach, A. Drobshoff,
M. Messerly, S. Mitchell, A. Brown, S.A. Payne
Lawrence Livermore National Laboratory

ABSTRACT

Laser guide stars are crucial to the broad use of astronomical adaptive optics, because they facilitate access to a large fraction of possible locations on the sky. Lasers tuned to the 589 nm atomic sodium resonance can create an artificial beacon at altitudes of 95-105 km, thus coming close to reproducing the light path of starlight. The deployment of multi-conjugate adaptive optics on large aperture telescopes world-wide will require the use of three to nine sodium laser guide stars in order to achieve uniform correction over the aperture with a high Strehl value. Current estimates place the minimum required laser power at > 10 W per laser for a continuous wave source, though a pulsed format, nominally 6 μs in length at ~ 16.7 kHz, is currently preferred as it would enable tracking the laser through the Na layer to mitigate spot elongation. The lasers also need to be compact, efficient, robust and turnkey. We are developing an all-fiber laser system for generating a 589 nm source for laser-guided adaptive optics. Fiber lasers are more compact and insensitive to alignment than their bulk laser counterparts, and the heat-dissipation characteristics of fibers, coupled with the high efficiencies demonstrated and excellent spatial mode characteristics, make them a preferred candidate for many high power applications.

Our design is based on sum-frequency mixing an Er/Yb:doped fiber laser operating at 1583 nm with a 938 nm Nd:silica fiber laser in a periodically poled crystal to generate 589 nm. We have demonstrated 14 W at 1583 nm with an Er/Yb:doped fiber laser, based on a Koheras single frequency fiber oscillator amplified in an IPG Photonics fiber amplifier. The Nd:silica fiber laser is a somewhat more novel device, since the Nd^{3+} ions must operate on the resonance transition (i.e. $^4F_{3/2}$-$^4I_{9/2}$), while suppressing ASE losses at the more conventional 1088 nm transition. Optimization of the ratio of the fiber core and cladding permits operation of the laser at room temperature by minimizing the 1088 nm gain, along with induced bend loss. A 938 nm seed beam is provided by a 0.2 W diode laser, frequency broadened to 400 MHz by DC modulating the diode. This seeds a two stage double-clad, Nd:doped fiber amplifier, producing 16 W of 938 nm light with M^2~ 1.05. Over 3.5 W at 589 nm in continuous wave (CW) format has been generated by sum-frequency mixing the two lasers in periodically poled potassium dihydrogen phosphate (PPKTP).

To convert the system to a pulsed format, we added amplitude modulators after both the 1583 nm and 938 nm oscillators and a pre-amplifier in each line to restore the average power to the level prior to modulation. Frequency mixing is simplified by using a pulsed format as the higher peak power facilitates more efficient conversion. To date we have demonstrated 3.8 W at 589 nm in periodically poled stoichiometric lithium tantalate (PPSLT) using a 1 μs pulse length and a 10% duty cycle. Additional bandwidth, pre-compensation for square pulse distortion (SPD) and polarization maintaining amplifier fiber is currently being implemented to enable scaling to higher output power and lower repetition rate. Details of these experiments, system design and performance will be presented.

1. INTRODUCTION

High power lasers capable of generating 589 nm for efficient excitation of the D2 line of the Na atom are of great interest to the astronomical scientific community for their use as laser guide stars in adaptive optics systems. These lasers are focused onto the sodium layer of the atmosphere, which is approximately 10 km thick and located approximately 90 km above the surface of the earth. In this layer of the atmosphere there is a relative abundance of alkali vapor, particularly Na, deposited by meteorites. A high power 589 nm laser focused on this layer of the atmosphere generates a spot of resonant fluorescence that appears to a telescope as an artificial star. This artificial star can be re-imaged through the telescope onto a Shack-Hartmann wavefront sensor to provide significant details about the atmospheric optical distortion. This information can then be fed back to a deformable mirror in the telescope optical train to correct for the phase errors and significantly improve the resolution of a large telescope. A natural star can also serve this purpose, but suitably bright natural stars occur only within about 10% of the visible sky. Laser generated guide stars enable expansion of adaptive optic techniques to greater than 60% of the visible sky.

As a result of the great improvement in telescope imagery from sodium laser guide stars, there has been a great deal of work recently in developing laser based adaptive optic systems. In particular, the Lick, Keck, Gemini North and South, Paranal, Palomar and Subaru observatories are all developing sodium laser guide star adaptive optic systems, as well as Starfire Optical Range. A number of laser technologies have been pursued in conjunction with this work. Dye lasers have been engineered to relative robustness and deployed at the Lick and Keck Observatory [1] and one is currently being deployed at the Paranal observatory [2]. Starfire Optical Range has deployed a 50 W CW single frequency laser based on sum-frequency mixing (SFM) 1319 nm and 1064 nm Nd:YAG lasers. ARFL developed this laser using a series of phase locked loops to generate the intense IR light needed for SFM and resonant cavity enhancement increases the frequency conversion efficiency in LBO to an acceptable level [3]. Coherent Technologies has developed a CW mode-locked laser system based on Nd:YAG lasers for the Gemini North Observatory [4]. The University of Chicago in collaboration with Caltech has developed and deployed a micro-macro pulse Nd:YAG SFM laser system for the Palomar Observatory [5]. However, all of these systems have a high degree of complexity and most require a laser technician to be on-call at the telescope to ensure reliable functioning of the laser. There is a desire for a more robust solution, such as would be provided by a suitable fiber laser. A fiber laser master-oscillator power amplifier configuration would also enable the possibility of generating specific pulse formats of interest to the adaptive optics community for gating out lower atmospheric Rayleigh scattering or tracking the laser pulse through the sodium layer to eliminate spot elongation effects. Concepts for multi-conjugate adaptive optics (MCAO) on thirty-meter class telescopes are dependent on the feasibility of sodium guide star lasers to achieve diffraction-limited image quality in the near IR over 1-2 arc minute fields of view.

To achieve projected performance for next generation extremely large telescopes (ELT), new laser and beam projection concepts must be developed with performance characteristics well beyond the current generation of systems. Current sodium lasers are sufficient for system development of the single laser case and near term MCAO systems, but are not adequate for ELTs. Innovations are needed to defeat the guide star elongation problem induced by the depth of the sodium layer. Possible approaches proposed to date include significantly higher-power laser systems, innovative pulse formats, up-link AO correction of the LGS to produce a smaller spot and/or a multiplicity of launch telescopes for each guide star location. Calculations indicate it is possible to operate the LLNL fiber technology in all of the pulse formats currently proposed to mitigate spot elongation in the sodium layer with adequate power. Currently the favorite format is a 3 μs pulse width at 16.7 kHz pulse rate, which results in only 1 pulse in Na layer at any given point in time. A specialized CCD is being developed by Beletic, et. al., to temporally resolve the propagation of the pulse through the Na layer, so the elongation of the image in the wavefront sensor due to the finite thickness of the Na layer can be calculated and corrected.

Some common requirements for lasers for this application are > 10 W of diffraction limited output power, wavelength of 589 nm locked to the sodium D2 line, bandwidth < 3 GHz (preferably less than 500 MHz), which is the Doppler broadened linewidth of Na in the upper atmosphere. The ability to generate up to 500 MHz is desirable in order to eliminate saturation effects in the Na layer, particularly in pulsed laser systems. The ability to run the laser in a pulsed mode is also desirable. We are developing fiber laser system to meet these requirements based on sum frequency mixing a 938 nm Nd^{3+} fiber laser with a 1583 nm Er^{3+} fiber laser (Fig. 1).[6]

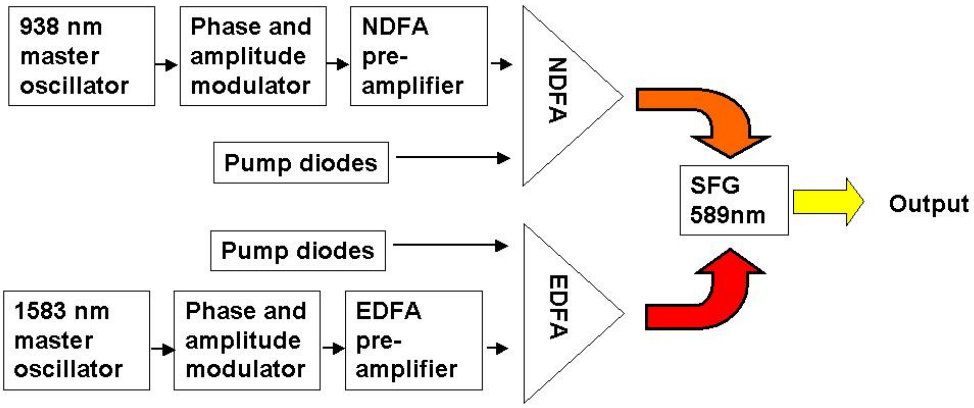

Fig. 1: Schematic of the LLNL sum frequency laser for generation of pulsed 589 nm guide star applications.

Our system sum frequency mixes 938 nm light with 1583 nm light to generate 589 nm light. A 938 nm diode laser master oscillator is amplitude and phase modulated, then amplified in a 2-stage neodymium doped fiber amplifier custom designed at LLNL[7]. A distributed feedback (DFB) fiber laser acts as the 1583 nm master oscillator. It is phase and amplitude modulated, then amplified in a simple erbium doped fiber preamplifier and an IPG 14 W power amplifier. The output of the 1583 nm and 938 nm lasers is collimated, combined in a dichroic and focused into a PPSLT crystal, where they sum-frequency mix to generate 589 nm light. The 938 nm and 1583 nm laser systems are described in detail below along with the sum-frequency mixing scheme.

2. NEODYMIUM FIBER LASER AT 938 NM

Our 938 nm fiber laser master oscillator is an Axcel Photonics 200 mW Fabry-Perot diode laser mounted in a standard diode laser mount with an integrated bias T. This diode conveniently lases in a single longitudinal mode at 938 nm with some adjustment of the wavelength possible via temperature control. In the final field deployable system, this will be replaced with an external cavity laser diode. The bias T permits modulation of the laser diode drive current with an RF noise source, which allows us to broaden the laser diode line width to up 500 MHz. This line width broadening is simultaneously verified with a grating-based optical spectrum analyzer and a Fabry-Perot optical spectrum analyzer. The diode laser master oscillator passes through an optical isolator, an acousto-optic modulator and pair of dichroic filters. The dichroic filters pass 938 nm, but reject 1088 nm and 808 nm that may be traveling backwards from the first 938 nm fiber amplifier. The light from the diode laser is then coupled through a lens into our 938 nm neodymium fiber amplifier chain. The amplifier chain consists of a first stage amplifier that brings the signal in the 1-4 W range, depending upon the duty cycle of the pulse modulation, and a power amplifier that brings the final power to 15 W.

Our 938 nm fiber amplifiers are based on our proprietary fiber design, which was custom fabricated for us by Nufern. The fiber core composition is critical to good performance at 938 nm. The core consists of silica, neodymium and germania with no other co-dopants. This composition has been shown [8] to provide a significant shift of the standard neodymium emission spectra in glass. The usual 1064 nm emission peak shifts to 1088 nm and the usual 915 nm emission peak shifts to 938 nm. Addition of any phosphorous, aluminum or other co-dopants shifts the spectra back to shorter wavelengths. As we are using the 938 nm in a sum frequency scheme with 1583 nm as the other wavelength, wavelengths shorter than 938 nm require a second wavelength beyond the reach of the erbium amplifier gain bandwidth. However, the use of this core composition strictly limits the doping concentration of Nd^{3+} in the glass to < 10 dB/m of absorption at 808 nm. For our narrow line width, high power application, we require a relatively short fiber amplifier with a large core area that is capable of output powers in the 20 W range at 938 nm, as well as suppression of amplified spontaneous emission and parasitic laser action at 1088 nm. We solved this problem by making the area of the fiber core large relative to the area of the pump cladding.[9]

The first stage amplifier has a 20 μm diameter core with a 0.06 NA. The fiber pump cladding is 125 μm in diameter and the fiber is 25 m long. The fiber is pumped by 35 W of 808 nm laser diode light that counter-propagates relative to the signal. The 808 nm light is coupled through a pair of dichroics that protect the pump laser from 938 nm light and 1088 nm light that might be generated by a Q-switch resulting from the inadvertent loss of the 938 nm seed beam. The fiber is coiled inside a water-cooled copper tube to an 8-cm diameter in a single layer. The tube ensures the fiber temperature remains constant, close to the ambient environment. At 938 nm, the power conversion efficiency from the pump wavelength to the signal wavelength in the Nd^{3+} fiber amplifier is in the 10-30% range. This results in significant amounts of heat being dumped into the fiber itself. Since the gain dynamics of the amplifier are sensitive to the fiber temperature, some level of cooling is required. The 938 nm transition is a 3-level transition the gain at that wavelength is affected by the absorption cross-section of the unexcited ion at 938 nm. The 1088 nm transition is a 4-level transition for which there is no ground state absorption. Fig. 2 (LHS) shows the 938 nm absorption cross-section of the Nd^{3+} ion in our glass composition. The models from which we designed our fiber assume the fiber is at room temperature. At higher temperatures, the absorption cross-section increases rapidly resulting in much more 1088 nm gain for the same gain at 938 nm. Fig. 2 (RHS) shows the effect of changing the temperature of the copper heat sink for the fiber coil. Lowering the temperature somewhat results in a significant efficiency increase at 938 nm.

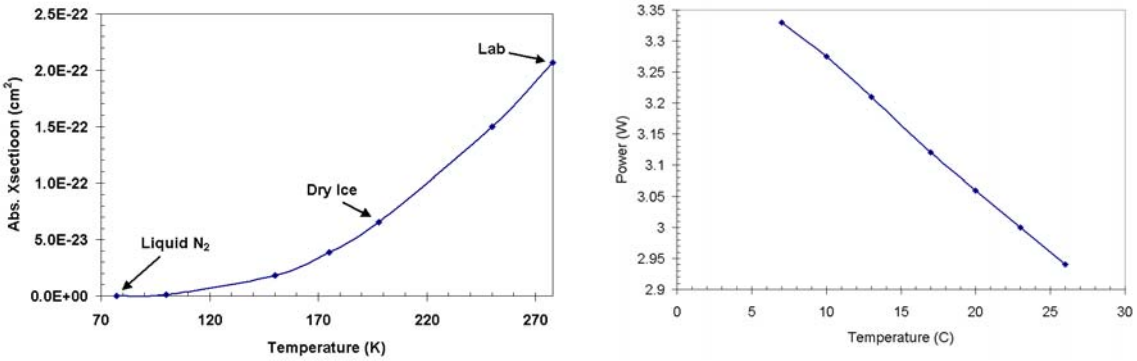

Fig. 2: Left hand side (LHS): calculated absorption cross-section at 938 nm vs. temperature; right hand side (RHS): output power of first stage 938 nm fiber amplifier vs. temperature of copper heat sink for fiber coil.

The light at the output of the first amplifier stage has $M^2 < 1.1$ and up to 3.5 W average power in CW mode. The light from the first stage is collimated, passed through a quarter and half waveplate to adjust the polarization state, a short pass filter to eliminate 1088 nm ASE from propagating into the next stage and an optical isolator to prevent feedback into the first stage. The 3.5 W is measured at the output of the optical isolator after passing through all the filters and waveplates. The second stage is constructed from a 40 m piece of Nd^{3+} fiber with same core composition as the first-stage fiber, but with a 30 μm, 0.06 NA core and 125 μm, 0.4 NA polymer coated pump cladding. This fiber is again coiled to 8 cm diameter and taped to the inside of a water-cooled copper pipe. The 20 μm-core fiber in the first stage, when coiled to 8 cm, effectively propagates a single mode of the wave-guide. The output of the laser diode is asymmetric and tends to excite higher order modes of the 30 μm-core fiber. It was difficult to find a precise bend radius for filtering out the higher order modes from the 30 μm core, thus a 20 μm-core fiber was chosen for the first stage, where it acts as a spatial filter ensuring single mode beam quality. This good quality beam is launched into the 30 μm-core, where it propagates stably as a single spatial mode with an output of $M^2 < 1.2$ and good transmission (> 85%) through an optical isolator. The second stage is pumped with a 90 W fiber-coupled laser diode with a 200 μm spot and 0.22 NA. This laser diode is coupled via lenses to the second stage fiber through dichroics that pass 808 nm and reject 938 nm and 1088 nm. The output of the second stage as a function of pump diode current (40 A→ 90 W) is shown in Fig. 3 (RHS). The total output power is shown along with power through a short pass filter (eliminating 1088 nm ASE) and the optical isolator. We also show the total power incident on the frequency conversion crystal, which accounts for loss in the telescope that sets the beam size and location of the waist, as well as the dichroic, which combines the 938 nm and 1583 nm beams. In Fig. 3 (LHS), we show a picture of the fiber coiled inside its copper block heat sink.

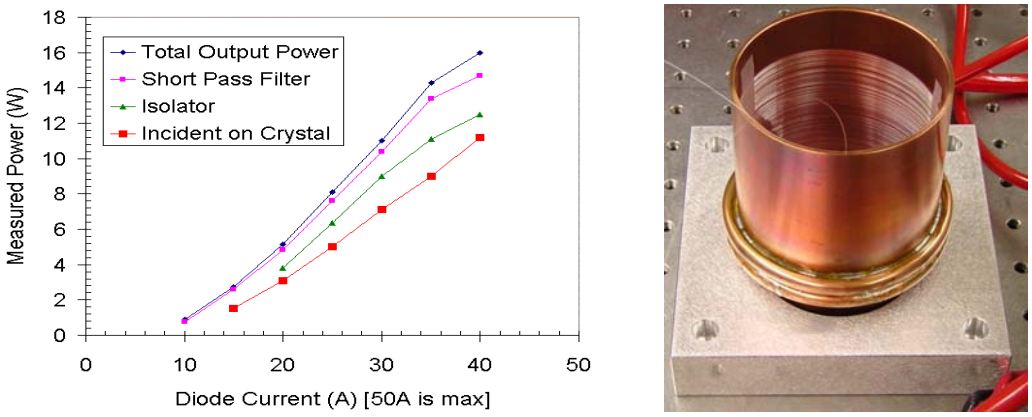

Fig. 3: Right hand side (RHS): Power vs. diode pump current of second stage neodymium fiber amplifier. Left hand side (LHS): water cooled copper heat sink to maintain fiber at room temperature in the presence of a strong pump laser.

We also investigated operation of this amplifier system in a pulsed format. First we sought to characterize the susceptibility of the system to stimulated Brillouin scattering (SBS). The response of fiber lasers to this effect is fairly well characterized at 1550 nm, where it is critical to the telecom industry, but less well characterized at shorter wavelengths. To this end, we first measured the bandwidth of our 938 nm diode laser as a function of the RF noise generator power. Then we pulsed the light entering the fiber amplifier. We measured the input signal, output signal, and return signal. We know the fiber length, core size and signal line width. From this information we were able to determine the power level for the onset of SBS as a function of the signal line width using equations 1-3 below [10].

$$P_0^{cr} = \frac{21 \cdot A_{eff}}{g_B(\Delta\nu) \cdot L_{eff}} \qquad (1)$$

where,

$$L_{eff} = \frac{1}{\alpha} \cdot \left[1 - e^{-\alpha \cdot L}\right] \qquad (2)$$

and,

$$g_B(\Delta\nu) = \frac{g_B}{1 + \frac{\Delta\nu}{\Delta\nu_B}} \qquad (3)$$

Here P^{cr}_0 is the input power to the amplifier for the onset of SBS, A_{eff} is the effective area of the core (which we take to be π times the mode field radius squared), L is the length of the amplifier, α is the loss or gain of the amplifier in nepers, $\Delta\nu$ is the bandwidth of the signal laser, g_B is the Brillouin gain and $\Delta\nu B$ is the Brillouin gain bandwidth. The latter two parameters are the fit parameters. In practice, the input power was held constant and the gain of the amplifier was increased until SBS was observed. The bandwidth, measured output power at the onset of SBS, the theoretical fit and fit parameters from this experiment are shown in Table 1.

Table 1: Left hand side: measured data from SBS experiment and theoretical fit to the data. Right hand side: fit parameters used to construct the theoretical output power in the last column on the right hand side table. All data was taken at 938 nm.

Bandwidth (MHz)	Measured Output Power (W)	Theoretical Output Power (W)
10	18.84	18.835
20	19.78	19.864
50	22.6	22.448
160	33.1	32.136
310	47.3	46.245

	Units	Theoretical Fit to data
g_B	m/W	$4X10^{-11}$
$\Delta\nu_B$	MHz	310

Using this knowledge, we have begun investigating the 938 nm laser in pulsed formats. To date we are operating at 100 kHz repetition rates so that square pulse distortion is minimal. Output data from the system, in essentially the same configuration as was used to generate the CW data set seen in Fig. 3, is shown in Fig. 4. For the data in Fig. 4, the laser was pulsed at 100 kHz with a 20% duty cycle (square waveform) and the signal line width was 500 MHz. 10 W of total output power was achieved. A spectral measurement (insert) shows that > 95% of the optical power measured is at 938 nm. Output power from the first stage was deliberately limited to 1.4 W, or about 17 dB of gain at 938 nm. At higher gain, the first stage began to show signs of Q-switching due to gain buildup at 1088 nm. Higher duty cycles performed equal or better than this. Due to limited gain per stage required to prevent Q-switching at 1088 nm, we cannot just turn up the gain per stage. As a result, we ran into problems at 10% duty cycle with low signal power. Compensation for square pulse distortion compensation, and possibly an additional stage of amplification, are being implemented to enable operation in this regime. However, the SBS modeling indicates that duty cycles down to 5% are feasible at 10 W average power levels.

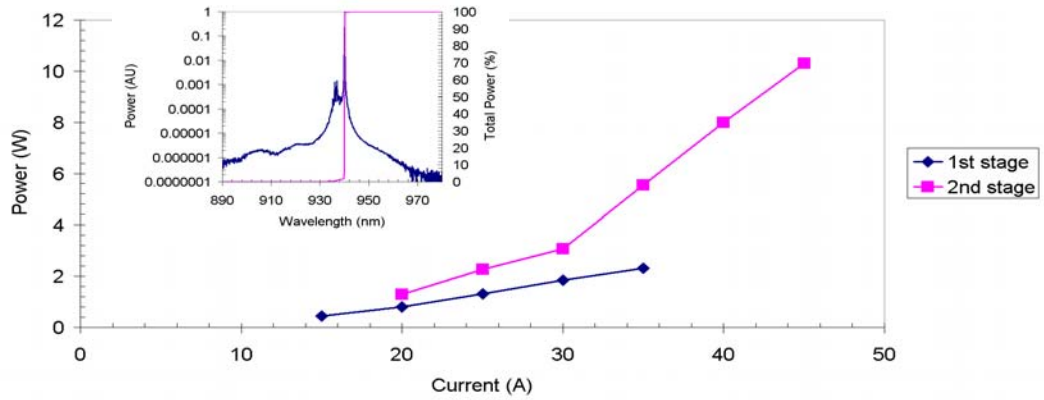

Figure 4: Power vs. pump diode current of 1st and 2nd stage fiber amplifiers in pulsed operation (20% duty cycle). Insert: Spectra at amplifier output and integration of spectra showing > 95% of the power is at the signal wavelength.

3. ERBIUM FIBER LASER AT 1583 NM

Our 1583 nm fiber laser system employed a Koheras DFB single frequency fiber laser as the master oscillator for several years, which was not polarization maintaining or very high power (~1-2 mW). This has been replaced with an upgraded Koheras oscillator with increased power and polarization maintenance. The light from the master oscillator is transmitted through an optical isolator and then is sent to a single mode pre-amplifier made from a single mode WDM, a 500 mW 980 nm pump laser, about 50 m of single mode erbium fiber, an optical isolator and a polarization controller. It is then transmitted through a lithium niobate phase modulator where it its bandwidth is increased to 500 MHz by driving the phase modulator at 100 MHz at several time V_{pi}. The phase modulated light is sent into a 90/10 PM fiber splitter with a polarizer on the 10% output that can be monitored with a power meter. Light through the polarizer is maximized using the polarization controller at the output of the pre-amplifier. The light from the 90% port is launched into a 14 W IPG PM fiber amplifier (model # EAR-15k-1583-LP-SF). The output of this module is a 5 mm collimated beam, which we down-collimate to the size required for our frequency conversion system after which the light is sent through a bulk optical isolator. We have also run this laser system as a pulsed laser by inserting an additional polarization controller and a PM lithium niobate amplitude modulator prior to the pre-amplifier.

Power vs. pump current and spectral output of the 1583 nm laser system run CW at 14 W is shown in Fig. 5. M^2 of the laser system was measured with a Coherent mode-master to be 1.05. The spectrum shows that > 98% of the output power is at the signal wavelength. We also tested the laser system run in a pulsed format. For this case, we ran the laser with signal modulated in a square waveform at 20% duty cycle and 100 kHz repetition rate. At 4 A pump current, the laser emitted > 10 W of average power with 95% of the power at the signal wavelength, as shown in Fig. 6. At 10% duty cycle, 8 W was produced prior to the onset of SBS. Additional phase modulation and square pulse distortion are being implemented to enable higher output power.

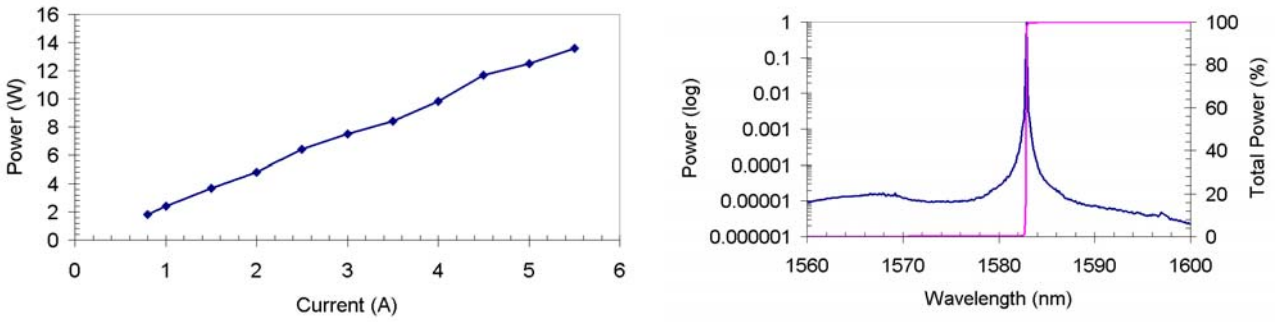

Figure 5: Left hand side: laser output power vs. pump laser current of the 1583 nm laser system run in CW mode. Right hand side: spectral output of the laser at 14 W. The pink "total power" line is the ratio of the power up to that wavelength to the total integrated power contained in spectra expressed as a percentage.

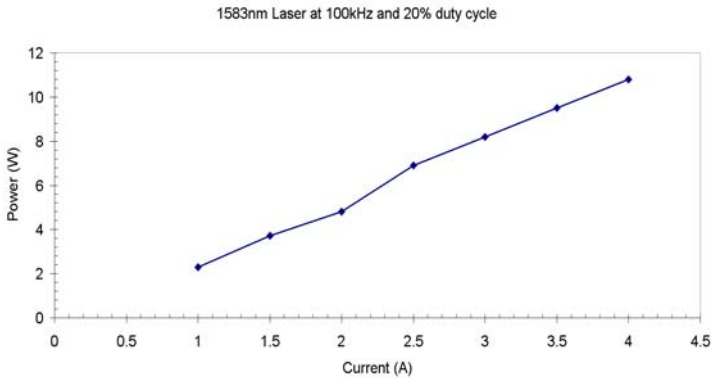

Fig. 6: The 1583 nm laser produced > 11 W at 20% duty cycle without signs of SBS.

4. SUM FREQUENCY MIXING

The 938 nm and 1583 nm lasers were sum frequency mixed in periodically poled materials. We examined both PPKTP and PPSLT. Sum frequency mixing is slightly more challenging than frequency doubling. This is because there are two independent beams with different wavelengths. The beams need to be co-linear throughout the frequency conversion crystals. As they are being focused through the crystal, they need to be co-linear at the lens, have the same confocal parameter and be focused to the same location in the crystal. Co-linearity is assured in our system by having 2 alignment irises about 1.5m apart on the table. By ensuring that each beam is well centered on both irises, we can assure the two beams are co-linear to < 1mrad. It is more difficult to ensure they have the same focus and confocal parameter.

Optimum conversion efficiency is achieved for Boyd-Klienman focusing [11], which indicates the crystal length should be about 2.7 times the confocal parameter. The confocal parameter is a function of the beam wavelength and diameter. An achromatic lens was used to make sure the beams focused to the same position. To ensure the beams have the same confocal parameter, the beam diameters need to be set to a ratio of 0.77. The latter condition was established by using a Coherent Mode Master to measure the beam diameter and location of the beam waist at the position on the table where we planned to put the focusing lens. Collimating telescopes were employed to adjust the diameter of the beams to the right size and to locate the beam waists at the focusing lens. This turns out to be a rather tedious process in practice. The Mode Master was very helpful in this endeavor in that it could quickly measure the beam diameter, divergence and location of the beam waist and beam waist diameter relative to the front plane of the instrument. We set the 1583 nm beam to 2.0 mm diameter with the waist within 50 cm of the focusing lens and the 938 nm beam was set to 1.5 mm diameter with the waist within 50 cm of the focusing lens. A 75 mm focal length lens was employed to focus the beams into our 3-cm long periodically poled crystals. This lens combination yields Boyd-Klienman focusing in our crystals, as predicted by calculations. A Pellan-Broca prism is used at the output of the crystals to separate the 589 nm light from the IR light prior to detection with a power meter.

The two lasers produced 2.7 W of 589 nm light in PPKTP in CW mode. The 589 nm power vs. total combined IR power curve is shown Fig. 7. Above 2.7 W the power rolled off and there was evidence of crystal degradation. The right hand side of Fig. 7 shows the oven, Pellan-Broca and a sodium cell fluorescing with the yellow glow from the 589 nm light. An additional 5X increase in conversion efficiency is expected by pulsing the IR lasers at 20% duty cycle. We switched to a PPSLT crystal, poled by Physical Sciences Incorporated, to avoid the damage issues observed in PPKTP. This 3 cm crystal was employed using the same beam and focusing conditions described above for the PPKTP crystal, yielding superior results. In the CW case the PPKTP had slightly lower conversion efficiency (3X vs. 5X). However, when we ran the system at 20% duty cycle, we were able to achieve 3.5 W of output power, as shown in Fig. 8. Again, about a 3X increase in converted power over the CW case was achieved. This slightly lower than the 5X expected increase due to a temporary polarization issue with the 1583 nm laser. At low 1583 nm power (~1W), we have achieved a 5X increase in conversion over the CW case, as expected, by careful tweaking of the polarization controllers. Following the upgrade of the 1583 nm laser, we successfully pulsed the system at 10% duty cycle and

reduced IR power, and achieved 3.8 W at 589 nm. There was no sign of damage in the PPSLT at the 3.5 W level over the timeframe of the experiment, which was albeit somewhat short (~30 min). We believe the PPSLT crystal will permit power scaling to 5-10 W average power at 589 nm.

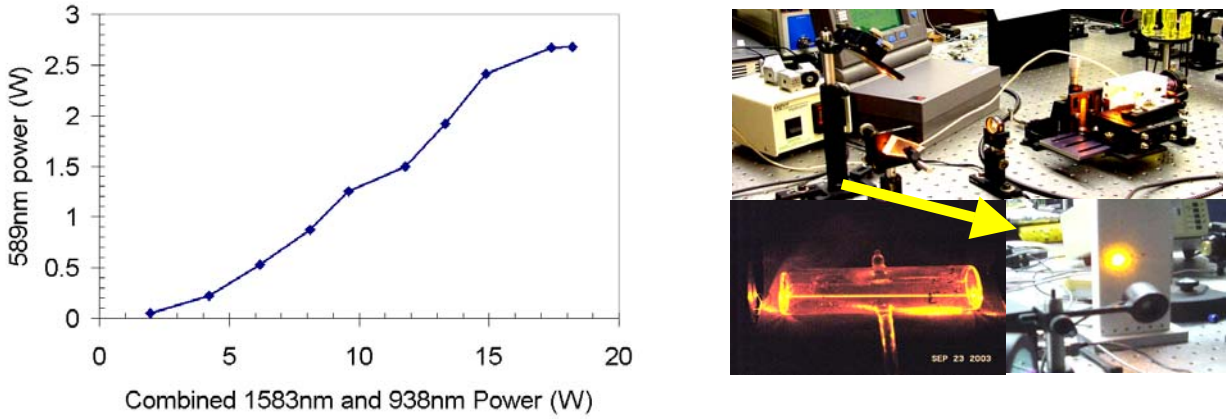

Fig. 7: Left hand side: 589 nm power vs. combined 1583 nm and 938 nm power for Boyd Kleinman focusing in a 3 cm long PPKTP crystal. Right hand side: pictures of 589 nm light from the experiment, oven, collimating lens and Pellan-Broca prism (top), fluorescence of the 589 nm beam in a sodium vapor cell (bottom left), low power 589 nm spot on a beam stop (lower right).

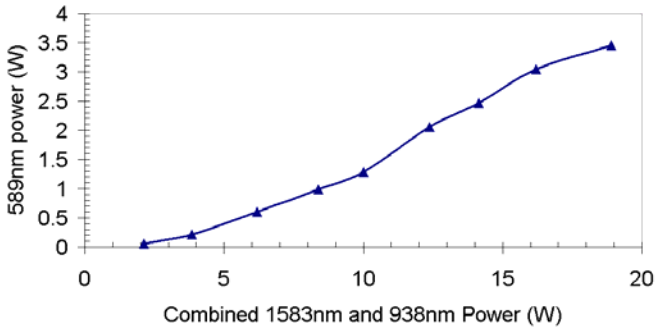

Fig. 8: 589 nm output power vs. combined 1583 nm and 938 nm power in PPSLT for 10%.

5. CONCLUSIONS

We are developing CW and pulsed 589 nm fiber lasers for sodium laser guide star applications. We have achieved >15 W of power at 938 nm with a Nd^{3+} based fiber amplifier system. We have measured the SBS gain and line width of our Nd^{3+} amplifier fiber to be 4 X 10^{-11} m/W and 310 MHz respectively. We have demonstrated laser operation at 100 kHz repetition rates with duty cycles as low as 10%, and believe high power at 5-10% duty cycles is possible, based on our SBS measurements. We have constructed a 14 W 1583 nm laser system from commercial components. This laser system is capable of operating in a pulsed format. We have achieved 3.8 W of 589 nm light via sum frequency mixing in a PPSLT crystal, and saw no signs of optical damage in the crystal during the course of our test.

The system is currently being upgraded for higher output powers, and will be engineered for field hardening flowing characterization experiments. The laser is currently scheduled to be installed on the Nickel telescope at Lick Observatory in late 2007 for use in a visible light adaptive optic demonstration.

This work was performed under the auspices of the U.S. Department of Energy by the University of California, Lawrence Livermore National Laboratory under contract No. W-7405-Eng-48, and has been supported in part by the National Science Foundation Science and Technology Center for Adaptive Optics, managed by the University of

California at Santa Cruz under cooperative agreement No. AST-9876783, the NSF Adaptive Optics Development Program, managed by the Associated Universities for Research in Astronomy and LLNL's Laboratory Directed Research and Development Office.

The PPSLT crystal discussed in this material was provided by Physical Sciences, Incorporated, as a result of work supported, in part, by the US Air Force Research Laboratory Directed Energy Directorate under Contract No.F29601-03-C-0044. Any opinions, findings, conclusions or recommendations expressed in this material are those of the authors and do not necessarily reflect the views of the US Air Force.

6. REFERENCES

1. D. M. Pennington, "Laser guided adaptive optics for high resolution astronomy," CLEO 2002, paper CMN5.
2. D. Bonaccini, W.K. Hackenberg, M. J. Cullum, E. Brunetto, T. Ott, M. Quattri, E. Allaert, M. Dimmler, M. Tarenghi,
3. A. Van Kersternen, C. Di Chirico, B. Buzzoni, P. Gray, R. Tamai, M. Tapia, "ESO VLT laser guide star facility," Proceedings of the SPIE, vol. 4494, pp. 276-289, (2002).
4. J.C. Bienfang, C.A. Denman, B.W. Grime, P.D. Hillman, G.T. Moore, J.M. Telle, "20W of continuous wave sodium D2 resonance radiation from sum-frequency generation with injection locked lasers," Optics Letters, vol.28, no. 22, pp. 2219-2221, (2003).
5. A.J. Tracy, A.K. Hankla, C.A. Lopez, D.C. Sadighi, N. Rogers, K. Groff, I. T. McKinnie, C. d"Orgeville, "High power solid state sodium beacon laser guide star for the Gemini North Observatory," Proceedings of the SPIE, vol. 5490, pp. 998-1009 (2004).
6. V. Velur, E. J. Kibblewhite, R.G. Dekany, M. Troy, H.L. Petrie, R.P. Thicksten, G. Brack, T. Trin, M. Cheselka, "Implementation of the Chicago sum frequency laser at Palomar laser guide star test bed," Proceedings of the SPIE, vol. 5490, pp. 1033-1040 (2004).
7. S.A. Payne, et al, "Synthetic guide star generation," US Patent # 6,704,331, issued 3/9/04
8. P. Dragic and G. Papen, "Efficient amplification using the $^4F_{3/2}$-$^4I_{9/2}$ transition in Nd:doped silica fiber," IEEE Phot. Tech. Lett. 11, 1593-1595 (1999). 9. J.W. Dawson, et. al, "938 nm fiber laser," US Patent #7038844, issued 5/2/2006.
10. J.W. Dawson, R. J. Beach, A. Drobshoff, Z.M. Liao, D.M. Pennington, S.A. Payne, L. Taylor, W. Hackenberg, D. Bonaccini, presented at Advanced Solid State Photonics, Santa Fe, NM, 2004.G.P. Agrawal, "Non-linear fiber optics, 2nd Edition", Academic Press 1995.
11. G.D. Boyd and D.A. Kleinman "Parametic Interaction of Focused Gaussian Light Beams", *J. of Appl. Phy.*, Vol. 39, No. 8, 3597-3639 , July 1968.